Journal of Photonics for Energy

PhotonicsforEnergy.SPIEDigitalLibrary.org

Silver- and copper-modified decahedral anatase titania particles as visible light-responsive plasmonic photocatalyst

Marcin Janczarek
Zhishun Wei
Maya Endo
Bunsho Ohtani
Ewa Kowalska

SPIE.

Marcin Janczarek, Zhishun Wei, Maya Endo, Bunsho Ohtani, Ewa Kowalska, "Silver- and copper-modified decahedral anatase titania particles as visible light-responsive plasmonic photocatalyst," *J. Photon. Energy* **7**(1), 012008 (2016), doi: 10.1117/1.JPE.7.012008.

Silver- and copper-modified decahedral anatase titania particles as visible light-responsive plasmonic photocatalyst

Marcin Janczarek,[a,b] Zhishun Wei,[a] Maya Endo,[a] Bunsho Ohtani,[a] and Ewa Kowalska[a,*]

[a]Hokkaido University, Institute for Catalysis, N21 W10, 001-0021 Sapporo, Japan
[b]Gdansk University of Technology, Department of Chemical Technology, G. Narutowicza 11/12, 80-233 Gdansk, Poland

Abstract. Decahedral anatase particles (DAPs) with eight equivalent (101) facets and two (001) facets were prepared by the gas-phase process. Monometallic and bimetallic photocatalysts were prepared by photodeposition of silver and copper on DAP. It was found that the method of metal deposition (sequential/simultaneous) is crucial for resultant properties and thus for photocatalytic performance. The fastest hydrogen evolution during metal deposition was observed for copper deposited on premodified DAP with silver (DAP/Ag/Cu), probably due to partial coverage of silver with fine clusters of Cu and thus facilitation of proton adsorption and reduction on well-dispersed Cu nanoclusters. Although DAP/Ag/Cu exhibited the fastest rate of hydrogen evolution, single-modified DAP with silver exhibited the best performance for oxidative decomposition of organic compounds under vis irradiation. [DOI: 10.1117/1.JPE.7.012008]

Keywords: photocatalysis; plasmonic nanoparticles; facetted anatase; titania morphology; decahedral anatase particles.

Paper 16061SS received May 30, 2016; accepted for publication Aug. 31, 2016; published online Sep. 21, 2016.

1 Introduction

Visible light-responsive photocatalysts have been considered as future materials which could help to solve emergency human problems concerning energy demand, drinkable water, and a clean environment.[1–4] Among them, modified titania photocatalysts have been the most extensively investigated since bare titania has often been found to be the best heterogeneous photocatalyst, due to high photocatalytic activity, availability, cheapness, stability, and negligible toxicity (i.e., due to the toxicity of nanomaterials).[5–8] Despite these advantages, the broad application of titania is still limited to world regions with a high intensity of solar radiation, due to its wide bandgap (ca. 3.0 to 3.2 eV depending on polymorphic form), and thus the necessity of being excited with UV irradiation.

Therefore, titania has been surface modified with organic and inorganic compounds,[9–11] and doped with various cations and anions,[11–14] which caused either narrowing of its bandgap[15] or photoinduced charge transfer between the titania and modifier.[16–18] It must be pointed out that modification could significantly influence the photocatalytic performance under UV irradiation, and in some cases, a decrease in photocatalytic activity has been observed since modifiers/dopants could also work as recombination centers for electrons and holes. Noble metals are one of the most extensively studied surface modifiers since they significantly inhibit the e^-/h^+ recombination under UV irradiation working as an electron sink,[19–23] and they can activate titania toward visible light irradiation due to localized surface plasmon resonance (LSPR), thus being

*Address all correspondence to: Ewa Kowalska, E-mail: kowalska@cat.hokudai.ac.jp

so-called "plasmonic photocatalysts."[24–26] Although application of noble metals as an electron sink under UV irradiation was started almost 40 years ago,[19] the use of plasmonic properties for photocatalysis under visible light is quite new,[27] which means that opposite results have been published, e.g., on the mechanism [charge transfer (mainly electron,[27–31] but also simultaneous hole transfer has been reported[32]), energy transfer,[33–35] and plasmonic heating[36–38]] and on decisive factors for photocatalytic performance (size and shape of plasmonic NPs and properties of the support).[39–44] Despite contrary results, a common conclusion can be drawn, i.e., the morphology of photocatalysts (properties of metallic deposits, semiconductor, and interactions between them) is decisive for both photocatalytic activity and the mechanism.[45] For example, a slight change in morphology of trilayered gold (core)/silver/titania nanorods resulted in a change of the mechanism from electron transfer to energy transfer (with an increase in titania thickness).[44] It should also be pointed out that a large majority of the studies has been performed for commercial support of noble metals, often on titania P25 (nonuniform mixture of anatase, rutile, and amorphous phases),[46,47] consisting of various impurities, irregular morphology, and being highly heterogeneous, where possible participation of various components and defects in resultant overall photocatalytic performance cannot be neglected. Therefore, in this study faceted anatase titania particles [decahedral anatase particles (DAPs) with eight (101) facets and two (001) facets] of well-controlled morphology and thus high photocatalytic activity were used as a support for nanoparticles of noble metals. Silver (Ag) and copper (Cu) were selected for this study, due to their advantageous prices (in comparison to gold and platinum) and future possible application for microorganism inactivation, as their antimicrobial properties have been known since ancient times, and nowadays the application of Ag and Cu in the form of various nanostructures has been intensively investigated.[48–53]

2 Experimental Details

DAPs were prepared by the gas-phase method, as reported elsewhere.[54] In brief, DAPs were prepared from titanium(IV) chloride ($TiCl_4$) and oxygen by rapid heating and quenching of the gas reaction mixture, which hindered the formation of perfect anatase crystals [octahedral anatase particles (OAPs)].[55] $TiCl_4$ was fed continuously to a vaporizer heated at 453 K through which argon passed to introduce $TiCl_4$ into a quartz tube set in an infrared furnace. Oxygen stream, coaxial with central $TiCl_4$ stream, was fed at 473 K. The central part of the quartz reactor tube was wrapped with platinum foil, and only this part was heated to 1373 K. DAP containing powder collected from the quartz tube and the glass fiber filter in the downstream were used for metal modification.

Silver and copper (2 wt. % in respect to titania) were photodeposited on titania in a sealed and deaerated (15 min Ar prebubbling) suspension of DAPs (500 mg) containing methanol (25 mL, 50 vol. %) and an aqueous solution of noble metal ($AgNO_3$, $CuSO_4 \cdot 5H_2O$) under UV/vis irradiation [high-pressure mercury lamp of 22-mW light intensity, under magnetic stirring (500 rpm) in a thermostated water bath (298 ± 5 K), set-up shown and described elsewhere[56]]. During the irradiation, the amount of generated hydrogen in the gas phase was measured every 15 min by gas chromatography (GC-TCD). The obtained metal-modified DAPs were centrifuged, washed three times with methanol and six times with Milli-Q water, and freeze-dried. Bimetallic-modified DAPs were prepared by simultaneous (codeposition) and sequential photodeposition of metals, i.e., DAP/Ag-Cu (codeposited), DAP/Ag/Cu (first Ag was deposited on titania and then Cu) and DAP/Cu/Ag (first Cu and then Ag). Details of the photodeposition method were presented previously.[57,58] The codes of samples were defined as DAP (anatase sample composed mainly of DAPs), DAP/Ag (silver deposited on DAP), DAP/Cu (copper deposited on DAP), DAP/Cu/Ag (silver deposited on DAP/Cu), DAP/Ag/Cu (copper deposited on DAP/Ag), and DAP/Ag-Cu (copper and silver codeposited on DAP).

Properties of samples were analyzed by diffuse reflectance spectroscopy (DRS; JASCO V-670 equipped with a PIN-757 integrating sphere), X-ray powder diffraction (XRD; Rigaku intelligent XRD SmartLab with a Cu target), X-ray photoelectron spectroscopy (XPS; JEOL JPC-9010MC with MgKα X-ray), scanning electron microscopy (SEM; JEOL JSM-7400F), and scanning transmission electron microscopy (STEM) equipped with an energy-dispersive

X-ray spectroscopy (STEM-EDS, HITACHI HD-2000).[54,59] For DRS analysis, barium sulfate and bare facetted anatase (DAP) were used as references.

Photocatalytic activity was tested for (1) decomposition of acetic acid (5 vol. %) under UV/vis irradiation (set-up used for metal photodeposition) and (2) oxidation of 2-propanol (5 vol. %) under vis irradiation [for two irradiation ranges: $\lambda > 420$ nm and $\lambda > 450$ nm: Xe lamp, water IR filter, quartz mirror, and cut-off filter Y45 and Y48, respectively (vis light intensity: 250 to 350 μW, lamp spectrum, and set-up shown previously)[42,56]]. Amounts of liberated (1) carbon dioxide in the gas phase and (2) acetone in the liquid phase (after powder separation) were determined by gas chromatography (GC-TCD and GC-FID, respectively), details shown elsewhere.[28]

3 Results and Discussion

3.1 *Preparation of Mono- and Bimetal-Modified DAP*

DAP was modified with NPs of Ag and Cu by the photodeposition method, and the data obtained for hydrogen evolution during photodeposition are shown in Fig. 1. Photoreduction of cations by photogenerated electrons on the surface of an irradiated semiconductor in the presence of a hole scavenger is one of the oldest and most often used methods for preparation of metal-modified semiconductors.[19,60–62] The fastest hydrogen evolution (the shortest induction period of ca. 7 min) was observed for Cu deposition on DAP. The induction period (intersection with the x-axis), during which NPs of noble metal are formed, differs depending on the noble metal and properties of titania. For example, photodeposition of Pt and Au is very fast with often undetectable induction periods (almost linear evolution of hydrogen from the beginning of irradiation).[50,57,58,63,64] However, for less noble metals, a longer irradiation time is necessary to reduce respective cations and to form NPs, e.g., 8 min for Cu and 45 min for Ag (during deposition on OAPs).[65] Cu is known for its stronger than Ag activity for methanol dehydrogenation due to its larger work function [4.61 to 4.67 eV (Ref. 66) and 4.14 to 4.46 eV (Ref. 67), respectively].[50,65] The difference between the metal work function and the electron affinity of titania (3.41 to 4.5 eV)[68–71] is decisive for generation of a Schottky barrier (the electronic potential barrier formed at the metal–semiconductor heterojunction), i.e., the greater the difference between the electron affinity of titania and the work function of metal is, the higher is the Schottky barrier. Additionally, the higher the Schottky barrier is, the higher is the transfer and trapping of photogenerated electrons by metal,[72] and thus the higher is the hydrogen generation rate. DAP/Cu/Ag and DAP/Ag-Cu bimetallic photocatalysts showed much lower activity than that of Cu-modified DAP. The poor activity of a codeposited sample (worse than expected: resultant reaction rate between that of two single-modified samples) is probably caused by possible formation of an AgCu alloy [Positive shift of XPS peak for Ag $3_{d5/2}$ from 368.1 to 368.2 eV for DAP/Ag and DAP/Ag-Cu, respectively (as was proposed for Ag–Cu bimetallic nanoparticles.)[73]]. An increase in the overvoltage toward the hydrogen evolution reaction was reported for an AgCu alloy electrode in comparison to electrodes composed of single metals (a silver electrode and a copper electrode), which was surprising since silver and copper have

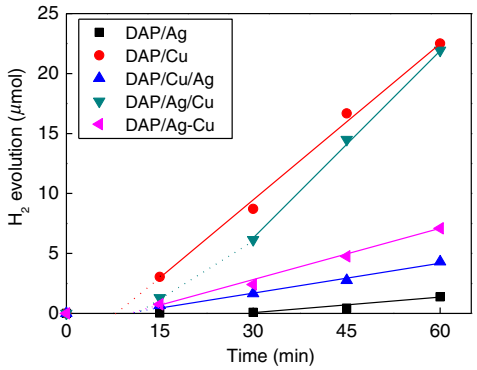

Fig. 1 Hydrogen evolution during photodeposition of metals on DAP sample.

similar properties concerning the overvoltage.[74] Therefore, a probably larger overvoltage for hydrogen evolution could be the reason for the low level of photocatalytic activity of the DAP/Ag-Cu sample. The DAP/Cu/Ag sample exhibited the lowest activity among bimetallic samples. It is thought that sequential deposition should result in partial coverage of one metal by another since during this deposition, NPs of predeposited metal (here Cu) are negatively charged (as they are an electron reservoir). Similarly, in the case of silver photodeposition on gold-modified titania, the formation of core(Au)-shell(Ag) was reported.[58] Thus, partial deposition of Ag on the surface of Cu (DAP/Cu/Ag) inhibited proton adsorption on the surface of Cu NPs and, consequently, in hydrogen evolution. Interestingly, sequential deposition of Cu on DAP/Ag (DAP/Ag/Cu) resulted in the highest rate of hydrogen evolution among all samples (0.53 μmol min^{-1} versus 0.04, 0.08, 0.14, and 0.44 μmol min^{-1} for DAP/Ag, DAP/Cu/Ag, DAP/Ag-Cu, and DAP/Cu, respectively). Although the induction period was slightly longer than that for single Cu deposition (DAP/Cu), since Ag (present on titania surface) disturbed in reduction of Cu(II), the linear evolution of hydrogen after 30 min of irradiation indicated an electronic interaction between two modifiers. To clarify the possible interactions detailed characterization of samples were performed.

3.2 *Characterization of Ag- and Cu-Modified DAP*

The color of samples was brown and violet during photodeposition of Ag and Cu, respectively, which confirmed that zero-valent metallic deposits were formed since LSPR of small spherical NPs of Ag and Cu appears at 410 to 430 (Refs. 75 and 76) and 560 nm,[77] respectively. In the case of sequential metal deposition, the samples took the color of the second metal, i.e., deposition of Cu on DAP/Ag resulted in DAP/Ag/Cu with violet color and deposition of Ag on DAP/Cu caused brown coloration of DAP/Cu/Ag. The color of sample during codeposition was dark gray. The color of dried samples (insets of Fig. 2) was different than that during photodeposition, which could be caused by surface oxidation of these less noble metals (In contrast, the color of Au- and Pt-modified titania did not change after contact with air.).[57,65] Similar observations on color change after sample drying were obtained for deposition of Ag and Cu on OAPs[65] and commercial titania samples.[42,48]

Photoabsorption properties (DRS spectra) are shown in Fig. 2. The intrinsic interband absorption of titania is observed at wavelengths shorter than 400 nm ($E_g \cong 3$ eV), as shown in Fig. 2(a). Slight photoabsorption observed for DAP at wavelengths longer than 400 nm could be caused either by impurity or a reduced form of titanium (Ti(III)). DAP possesses very high purity since only three compounds are used for its synthesis: $TiCl_4$, O_2, and Ar. Therefore, only chloride could be considered as its impurity. After synthesis, DAP was washed thoroughly with Milli-Q water and thus only a small content of chlorine (<0.5 wt. % of titania) was detected on the surface of DAP by XPS analysis. The possibility of formation of Ti(III) is also low since synthesis of DAP is performed in excess of oxygen in the system. On the other hand, the conditions of DAP synthesis, i.e., rapid heating and quenching of the reaction mixture (ca. 1-s residence time in the oven), which are necessary to avoid the formation of

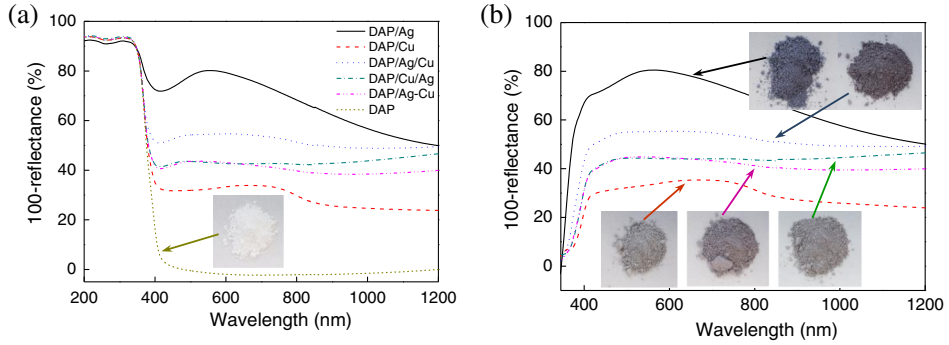

Fig. 2 DRS spectra of modified DAP samples taken with (a) $BaSO_4$ and (b) DAP as a reference. Inset: photograph of dried samples.

octahedron (thermodynamically favorable, OAPs) instead of decahedron, could result in formation of some lattice defects, e.g., reduced form of titanium [Ti(III)].

NPs of noble metals can absorb visible light as is clearly shown in Fig. 2(b). Two maxima in the LSPR peak could be observed for DAP/Ag, which indicates the high heterogeneity of silver deposits: fine nanosized NPs (LSPR at ca. 410 nm) and large particles (LSPR at ca. 590 nm).[49,78–80] The photoabsorption properties of Cu-modified samples are quite different than reported ones, where generally, due to rapid copper oxidation, no LSPR peak of Cu could be detected (no absorption at 400 to 600 nm), and a single broad peak at 600 to 1000 nm indicated the presence of CuO.[81,82] For a single DAP/Cu sample, the broad peak from 400 to 800 nm could be caused by: (1) the interfacial charge transfer (IFCT) from the valence band of titania to the Cu_xO ($X:1,2$) clusters at 400 to 500 nm, (2) the interband absorption of Cu_2O at 500 to 600 nm, (3) LSPR of zero-valent Cu at ca. 550 to 570 nm, and (4) $2E_g \rightarrow 2T_{2\,g}$ transitions of Cu^{2+} located in the distorted or perfect octahedral symmetry at 600 to 800 and 740 to 800 nm, respectively.[51,83,84] Considering the shape and width of the DRS peak of DAP/Cu with the maxima at ca. 700 nm, it is thought that copper could exist in all reported forms: Cu(0), Cu(I-II), Cu(I), and Cu(II). Interestingly, photoabsorption properties of bimetallic photocatalysts differed, and maxima at shorter wavelengths (ca. 510 nm) could indicate that Cu(I) is the predominant form in those samples.

Morphology of samples was investigated by microscopic observation, and exemplary STEM images for single-modified samples are shown in Fig. 3. It is clear that Cu forms small nanoclusters of ca. 2 nm, which are uniformly distributed on DAP. On the other hand, aggregation of silver results in the formation of polydispersed NPs (3 to 40 nm), which confirms the broad LSPR peak of silver (Fig. 2). Aggregation of Ag NPs results in the copresence of unmodified titania particles in the final product, as clearly shown in the right part of Fig. 3(a) (marked by a white, dashed rectangle), which should be crucial for the resultant photocatalytic activity.

To investigate morphology of bimetallic samples, STEM-EDS was applied, and exemplary images for DAP/Ag/Cu and DAP/Ag-Cu samples are shown in Figs. 4 and 5. In the DAP/Ag/Cu sample, Ag formed larger NPs than Cu, which was uniformly distributed on the surfaces of both titania and silver NPs. However, a few places with a high density of Cu were also observed, suggesting the formation of large Cu NPs, as shown in Fig. 4(b). It should be pointed out that larger NPs of Cu were only formed in the vicinity of Ag NPs. It is thought that the interaction between both metals during Cu deposition could result in the formation of aggregates of Cu since during photodeposition silver is negatively charged (working as an electron sink).

In contrast to DAP/Ag/Cu, no large Cu NPs were formed in the codeposited sample (DAP/Ag-Cu). This sample had uniformly distributed very fine (nanosized) Cu and Ag nanoclusters, as shown in Fig. 5. Interestingly, several large Ag deposits (>100 nm) were also observed in this sample, but they did not initiate the formation of large Cu NPs in their vicinity [Fig. 5(d)]. It is proposed that due to competition between the two metals during photodeposition, copper occupied the surface of titania first, forming either single nanoclusters or an alloy with silver. Similarly, copper hindered direct deposition of silver on titania. Therefore, large deposits of silver were also observed in this sample.

Surface composition of samples and oxidation states of elements were determined by XPS, and the data obtained are summarized in Table 1. Titanium, oxygen, carbon, silver, and copper

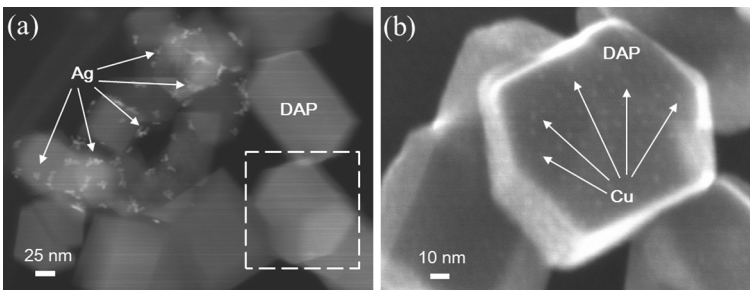

Fig. 3 STEM images of (a) DAP/Ag (marked region shows unmodified titania particle) and (b) DAP/Cu.

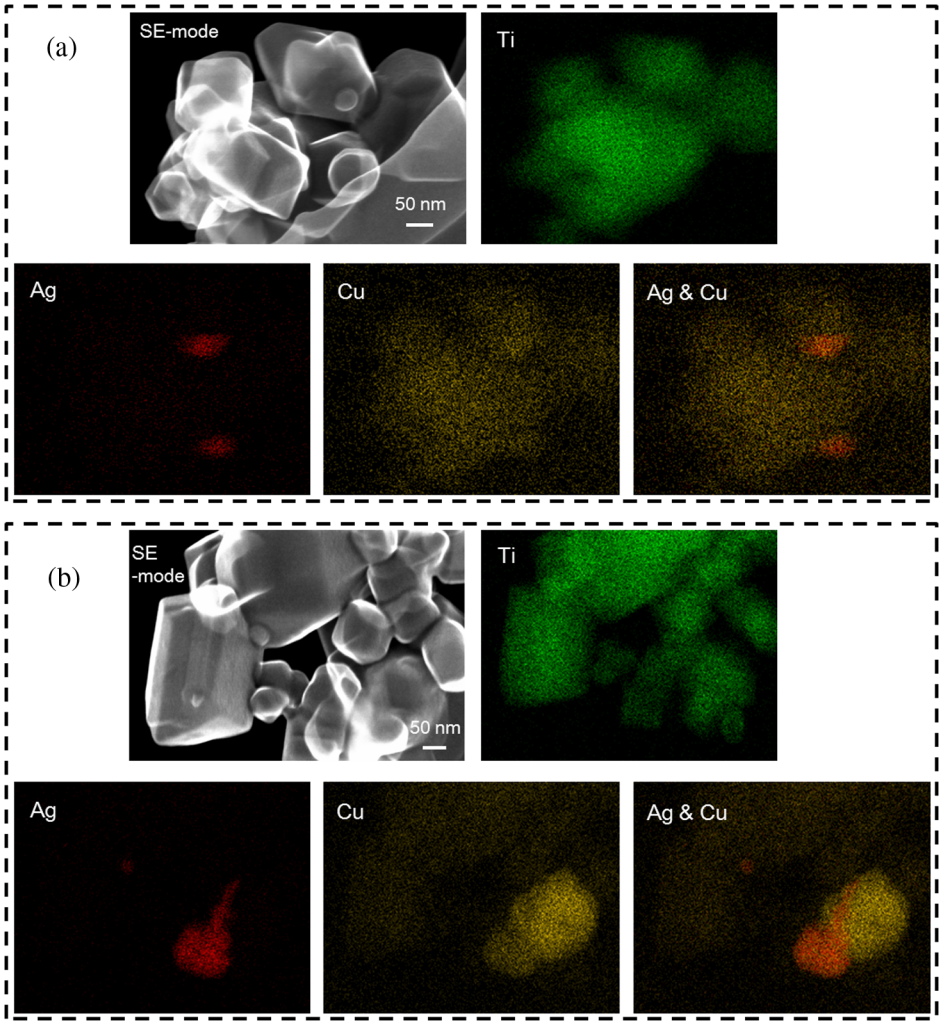

Fig. 4 (a) and (b) STEM images with respective EDS images of DAP/Ag/Cu taken at different view. Mapping colors: Ti, green; Ag, red; Cu, yellow; SE-mode, scanning mode of STEM.

were analyzed in detail, and a fraction of the oxidation states of elements from the deconvolution of XPS peaks is shown in Table 2. Exemplary XPS peaks for Ti $2p_{3/2}$, O 1s, C 1s, Cu $2p_{3/2}$, and Ag $3d_{5/2}$ of DAP/Cu/Ag sample are shown in Fig. 6. The ratio of oxygen to titanium exceeded two, reaching ca. 7.6 and 3.4 to 7.2 for bare and modified DAP samples, respectively. Enrichment of the titania surface with oxygen has been often reported, e.g., a ratio of 4.6 for titania samples prepared by the microemulsion method,[41] a ratio of 2.5 for titania prepared by laser ablation,[85] and a ratio of 2.2 to 5 for OAP prepared by HT (depending on duration of HT).[65] Significant excess of oxygen on the surface of DAP (7.6 ratio) is reasonable since anatase particles are formed under the continuous flow of oxygen. The deconvoluted oxygen peak indicates the presence of three forms of oxygen at ca. 529.4, 531.6, and 533.1 eV. The first peak is related to oxygen in the crystal lattice of TiO_2, the second peak to C═O, Ti_2O_3 and OH groups bound with two titanium atoms, and the third one is related mainly to hydroxyl groups bound to titanium and carbon (Ti—OH, C—OH).[86,87] The content of lattice oxygen on the surface of DAP amounted to only ca. 20%, thus the surface was mainly composed of hydroxyl groups (or other compounds containing oxygen, e.g., carbon dioxide from air). Modification of the DAP surface with NPs of noble metals resulted in a decrease in the content of hydroxyl groups (except for codeposited sample: DAP/Ag-Cu), which is reasonable since surface modifiers displaced other adsorbed species. This competition of adsorption on the titania surface between hydroxyl groups and metal deposits can be crucial for photocatalytic performance, especially in the case of reactions performed in organic media. For example, for cyclohexane oxidation, deposition of gold

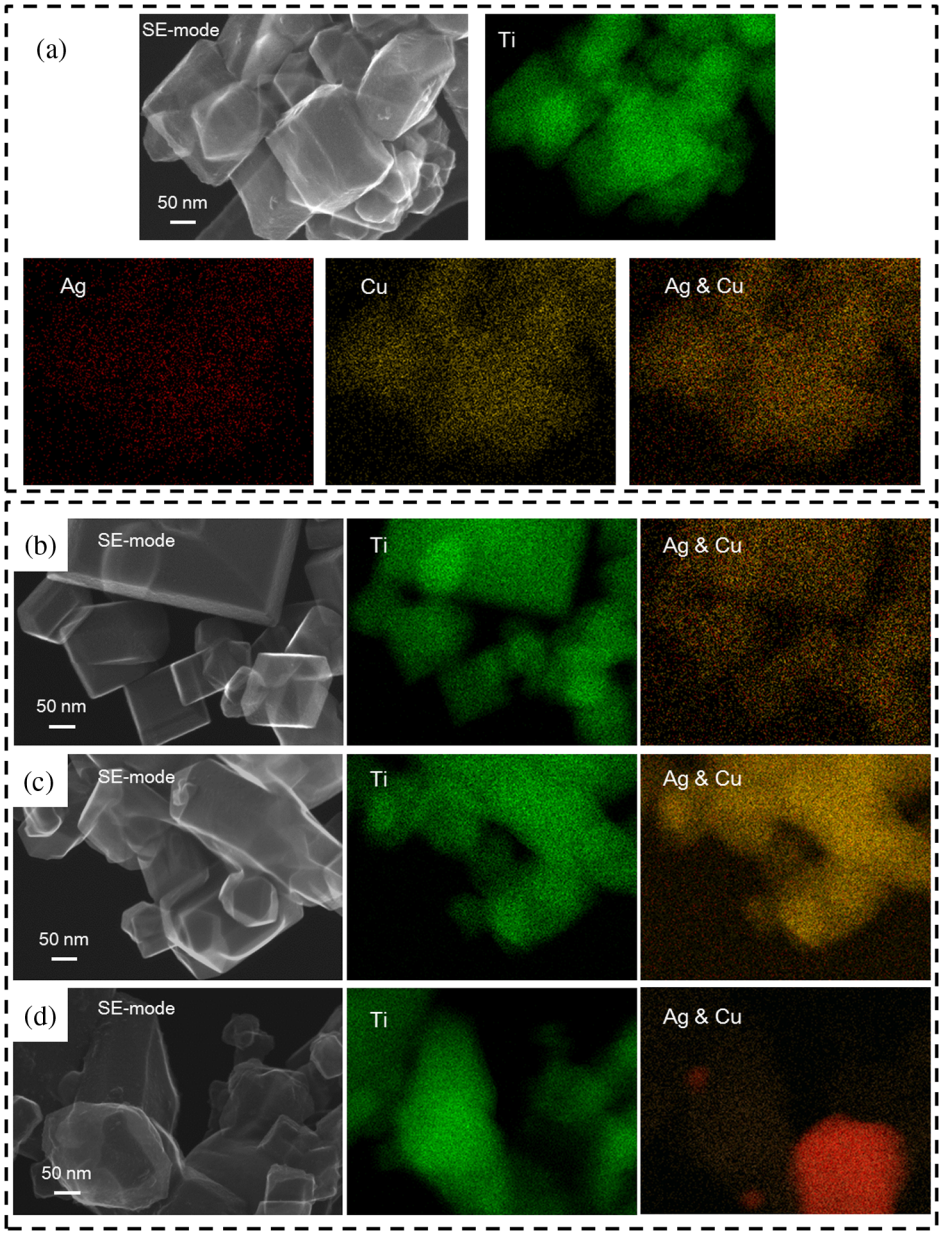

Fig. 5 (a)–(d) STEM images with respective EDS images of DAP/Ag-Cu taken at different view. Mapping colors: Ti, green; Ag, red; Cu, yellow; SE-mode, scanning mode of STEM.

NPs on the titania surface resulted in a decrease in the amount of available hydroxyl groups, which in consequence decreased the amount of generated hydroxyl radicals during irradiation and thus the efficiency of oxidation.[88] Slightly smaller content of lattice oxygen (TiO_2) in codeposited sample (DAP/Ag-Cu) indicates that some particular bimetallic nanostructure with surface oxygen enrichment was formed. Deconvolution of Cu and Ag peaks confirms that this sample differed significantly from others, having the largest Cu content, the smallest Ag content, the smallest content of Cu^{2+}, the largest content of Cu(0), and the largest content of Ag^{2+}. The most surprising aspect of the codeposited material is that it contains the largest fraction of Cu and the smallest fraction of Ag of any of the bimetallic composites: it is expected that the materials prepared by sequential deposition, DAP/Cu/Ag, and DAP/Ag/Cu, should have larger Ag and Cu content, respectively. Interestingly, the DAP/Ag-Cu sample has an even larger content of Cu on the surface (14 wt. %) than single-modified DAP with Cu (DAP/Cu, 12.9 wt. %). It is thought that during codeposition, segregation of two metals could result in the formation of a silver core and Cu discontinuous shell (fine Cu clusters deposited on the surface of silver). Similar metal

Table 1 XPS analysis of oxygen, titanium, carbon, silver, and copper for various DAP samples, and fraction of oxidation states of C from deconvolution of XPS peak of C 1s

	Content (at. %)					Ratio				C 1s (%)		
Samples	Ti	O	C	Ag	Cu	O/Ti	C/Ti	Ag (wt. %)	Cu (wt. %)	C—C	C—OH	C=O
Bare- and metal-modified DAP												
DAP	3.4	26.2	70.4	—	—	7.6	20.6	—	—	71.1	17.5	11.4
DAP/Ag	6.5	27.9	64.9	0.76	—	4.3	10.0	15.88	—	75.7	13.0	11.3
DAP/Cu	3.6	26.2	69.6	—	0.59	7.2	19.1	—	12.87	73.0	15.5	11.5
DAP/Ag/Cu	9.0	30.2	59.1	0.35	1.37	3.4	6.6	5.25	12.08	68.4	22.3	9.3
DAP/Cu/Ag	5.5	26.3	67.2	0.23	0.78	4.7	12.1	5.60	11.18	49.0	41.1	9.9
DAP/Ag–Cu	4.0	25.6	69.8	0.14	0.70	6.5	17.6	4.76	14.00	66.1	23.6	10.3

Table 2 Fraction of oxidation states of Ti, O, Cu, and Ag from deconvolution of XPS peaks of Ti $2p_{3/2}$, O 1s, Cu $2p_{3/2}$, and Ag $3d_{5/2}$

	Ti $2p_{3/2}$ (%)		O 1s (%)			Valent state (%)			Valent state (%)		
Samples	Ti^{4+}	Ti^{3+}	TiO_2	Ti-OH[a]	Ti-OH[b]	Ag^{2+}	Ag^{+}	Ag(0)	Cu^{2+}	Cu^{+}	Cu(0)
Bare- and metal-modified DAP											
DAP	98.0	2.0	20.8	44.2	35.0	—	—	—	—	—	—
DAP/Ag	98.2	1.8	33.3	46.4	20.3	0.53	89.50	9.97	—	—	—
DAP/Cu	96.1	3.9	25.5	37.5	37.0	—	—	—	12.8	82.0	5.2
DAP/Ag/Cu	100	0.0	27.2	29.6	43.2	5.0	67.6	27.3	16.1	82.8	1.1
DAP/Cu/Ag	96.7	3.3	28.8	33.2	38.0	1.0	82.7	16.3	5.6	93.7	0.7
DAP/Ag-Cu	100	0.0	19.7	38.7	41.6	6.7	83.3	10.0	2.9	89.0	0.7

[a]Ti-(OH)-Ti, Ti_2O_3, C = O.
[b]Ti-OH, C-OH.

segregation for Ag-Cu composites has already been reported, e.g., during radiolytic reduction–deposition of Ag and Cu on titania P25.[81] However, based on obtained STEM-EDS images, it is difficult to confirm/reject the possibility of formation of an Ag(core)-Cu(shell) due to the small sizes of metallic clusters (nanosized) uniformly dispersed on the support (Fig. 5). It is highly possible that the mixture of Ag-Cu alloyed nanoclusters, core–shell nanoclusters, and monometallic nanoclusters/NPs (nanoclusters of Cu and large deposits of Ag) could coexist in the codeposited sample.

NPs of silver and copper have positively charged surfaces with 1+ being the predominant form (Ag^{+} and Cu^{+}). Sequential deposition significantly influenced the form (charge) of predeposited metals, i.e., DAP/Ag/Cu has the highest content of zero-charged silver (27.3%) since at the beginning of Cu deposition, electrons from titania are sinking in predeposited silver, and subsequently deposited Cu stabilized Ag NPs. Similarly, a decrease in the content of 2+ charged Cu (from 12.8% to 5.6%) and increase in the content of 1+ charged Cu (from 82% to 93.7%) was observed in the case of sequential deposition of Ag on DAP/Cu.

Titanium in all samples existed mainly in Ti^{4+} form, e.g., 98% in DAP (details in Table 2). Deposition of metals slightly changed the surface composition of the sample, and the largest content of oxygen vacancies (Ti^{3+}) was observed for samples in which Cu was deposited first, e.g., ca. 3.9% in the DAP/Cu sample and ca. 3.3% in the DAP/Cu/Ag sample. On the

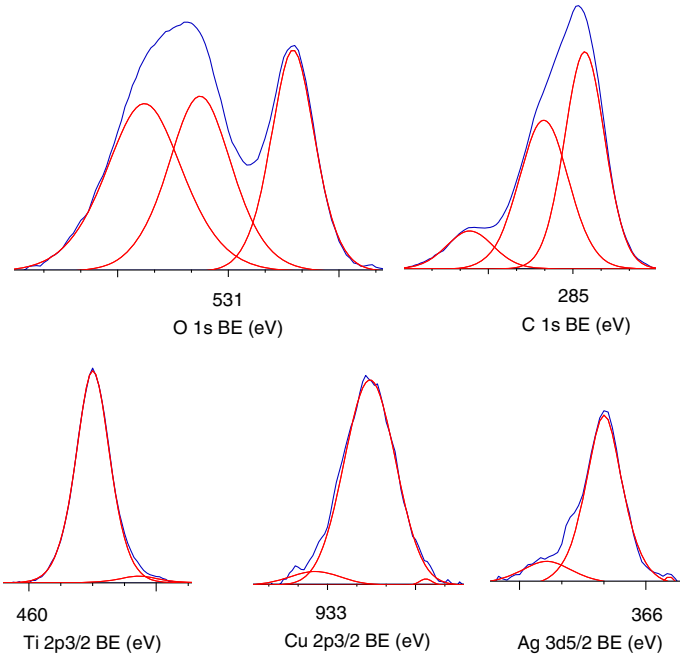

Fig. 6 XPS results for O 1s, C 1s, Ti 2p3/2, Cu 2p3/2, and Ag 3d5/2 for DAP/Cu/Ag sample.

other hand, deposition of silver decreased the content of Ti^{3+}, suggesting preferential deposition of silver on lattice defects. Similar behavior was proposed for gold NPs, which were preferentially formed on lattice defects of titania.[28,89]

3.3 *Photocatalytic Activity of Ag- and Cu-Modified DAP*

DAP modification with silver and copper resulted in significant enhancement of UV/vis photocatalytic oxidation of acetic acid, as shown in Fig. 7. DAP/Ag exhibited the highest photocatalytic activity, indicating that an enhancement in activity did not correlate with the work function of metals. Therefore, not only formation of the Schottky barrier (inhibition of e^-/h^+ recombination), but also other factors were crucial for overall photocatalytic performance. Previously, it was shown that the content of surface hydroxyl groups influenced the formation of reactive oxygen species (ROS), and thus photocatalytic activity.[90,91] For example, Cu/OAPs possessing the highest content of hydroxyl groups on its surface also exhibited the highest photocatalytic activity among other OAPs samples modified with Ag, Pt, and Au.[65] Interestingly, in this study, neither the work function of metal nor the content of hydroxyl groups correlated with photocatalytic activity, i.e., DAP/Ag has the highest activity despite the lowest content of

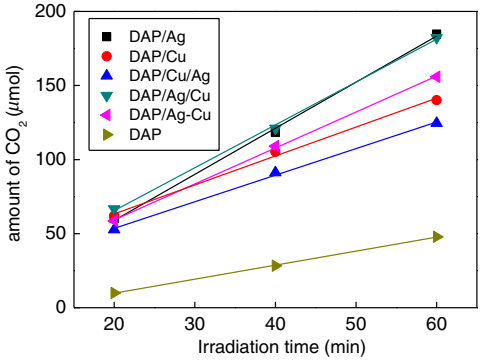

Fig. 7 Oxidative decomposition of acetic acid on bare and modified DAP with noble metals under UV/vis irradiation.

hydroxyl groups on the surface. In contrast to methanol dehydrogenation (anaerobic conditions), decomposition of acetic acid was carried out in the presence of oxygen. In this regard, the possible heterojunctions between oxides of noble metals (formed on the surface of metallic deposits) and titania could result in enhanced photocatalytic activity. Similar heterojunctions between titania and CuO, Cu_2O, Ag_2O, and AgO have already been proposed for inhibition of the recombination of charge carriers.[53,81,84,92] It is also possible that heterojunction CuO/Cu_2O-TiO_2 is less active than metal-modified titania Ag/TiO_2 or Ag-AgO/TiO_2. (Copper exists mainly in oxidized form, but silver coexists in metallic and oxidized form.) To clarify this matter, a series of photocatalysts possessing the same composition and being different only by the oxidation state of metals will be investigated in future research.

The two most active samples (DAP/Ag and DAP/Ag/Cu) differed significantly in their properties, i.e., DAP/Ag had the highest content of Ag^+ (89.5%) among all samples, whereas DAP/Ag/Cu had the lowest content of Ag^+ (67.7) and the highest content of zero-valent Ag (27.3%). Therefore, different mechanisms for both samples should be proposed, i.e., interparticle charge transfer between: (1) TiO_2 and Ag_2O for DAP/Ag, and (2) TiO_2-AgO/Ag-CuO/Cu_2O for DAP/Ag/Cu. The correlation between photocatalytic activities of bimetallic samples under anaerobic conditions (methanol dehydrogenation, Fig. 1) and aerobic conditions (Fig. 7) suggests that the morphology of bimetallic deposits is crucial for photocatalytic performance. Therefore, it is proposed that the most active sample (DAP/Ag/Cu) has Cu nanoclusters uniformly distributed on the surface of both titania and Ag NPs (Fig. 4). However, participation of larger NPs of Cu, deposited in the vicinity of Ag NPs, in the overall photocatalytic performance could not be neglected and will be investigated in detail in our future study.

Photocatalytic activity under visible light irradiation was first tested for irradiation at wavelengths longer than 420 nm to ensure inactivity of bare titania and to keep overall plasmonic properties of silver. Photocatalytic activity of modified samples [Fig. 8(a)] generally correlated with their photoabsorption properties (Fig. 2). DAP/Ag sample had the strongest absorption of visible light and its photocatalytic activity was the highest. However, observed photocatalytic activity of bare DAP under irradiation with a visible light was surprising and made the discussion on the photocatalytic performance of other modified samples, which showed lower photocatalytic activity than that of DAP, difficult suggesting that those modifiers hindered the intrinsic activity of bare DAP (This vis-response could be caused by the presence of adsorbed Cl^- or Ti^{3+}, since small conductivity for bare DAP samples was observed even up to 545 nm, and this phenomenon will be investigated in detail in our future study.). Therefore, activity tests were repeated for a narrower range of irradiation by using another cut-off filter (Y48) to ensure the transmission of light with wavelengths longer than 450 nm [Fig. 8(b)]. Indeed, application of longer wavelengths of irradiation eliminated the visible response of bare DAP. The photocatalytic activity of bimetallic samples (DAP/Ag/Cu, DAP/Cu/Ag, DAP/Ag-Cu) corresponds with the photoabsorption properties presented in Fig. 2. DAP/Ag showed the highest visible activity among tested samples. Interestingly, DAP/Cu showed slightly higher activity than bimetallic samples. Similar behavior was observed for other plasmonic photocatalysts (Au-Ag, Au-Cu, Ag-CuO) under visible light irradiation, i.e., decrease in activity after addition

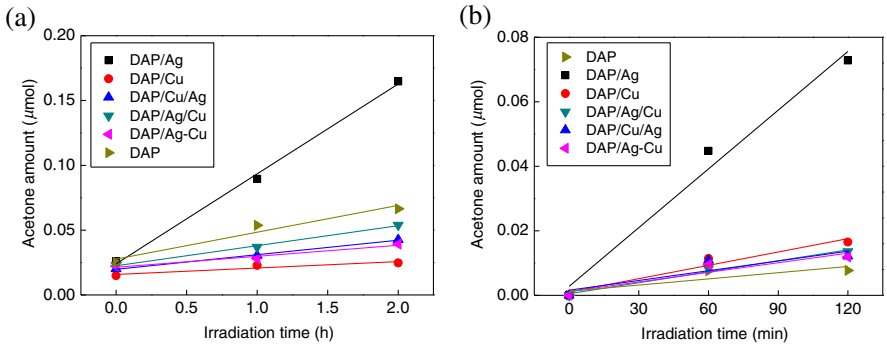

Fig. 8 Photocatalytic activity of bare and modified DAP under visible light irradiation: (a) $\lambda > 420$ nm and (b) $\lambda > 455$ nm.

of the second modifier.[58,81,93,94] For example, in the case of bimetallic photocatalysts containing silver and gold, single-modified samples showed higher photocatalytic activity (either TiO_2/Au or TiO_2/Ag depending on titania support properties) than bimetallic photocatalysts in which two metals formed a bimetallic nanostructure, e.g., core–shell.[58] Only photocatalysts with NPs of both metals separately deposited on titania (Ag NPs and Au NPs) showed higher photocatalytic activity due to the ability of absorption of more photons by LSPR of two metals (different positions of LSPR). It was proposed that the deposition of two metals close to each other (bimetallic nanostructure) resulted in electron transfer from one metallic deposit to another one (recombination of charge carriers), instead of being transferred to the conduction band of titania. Similarly, modified titania P25 with Ag and CuO showed the best photocatalytic performance for single-modified titania with CuO, then with Ag, and finally with bimetallic NPs.[81] Although, in this study, opposite performance of single-modified samples was noticed, i.e., higher activity of TiO_2/Ag than that of $TiO_2/Cu(Cu/Cu_2O/CuO)$, all bimetallic photocatalysts exhibited worse photocatalytic activities than monometallic ones, which could indirectly support the mechanism of action of plasmonic photocatalysts through the charge transfer mechanism rather than energy transfer one. The opposite performance of monometallic photocatalysts (activity: $TiO_2/Ag > TiO_2/Cu$) than the reported one (activity: $TiO_2/Cu > TiO_2/Ag$), could result from the properties of copper where Cu was mainly in the form of CuO. Therefore, the heterojunction between two semiconductors, CuO and TiO_2, could result in enhanced photocatalytic performance. (It should be pointed that P25 consists of anatase and rutile, which influences the properties and photocatalytic activity of resultant photocatalysts by either preferential deposition of metal NPs at the anatase/rutile junction or by charge transfer between two crystalline components and/or modifiers.) In this study, Cu is mainly in the form of Cu_2O. Therefore, it is proposed that for activation of titania under visible light Cu in the form of CuO is more recommended.

4 Summary and Conclusions

Facetted anatase titania particles with a decahedral crystal shape were intended for modification by silver and copper. Photodeposition of silver and copper on the DAP surface was successful and monometallic and bimetallic photocatalysts were obtained. The type of the selected method of metal deposition determines the resultant parameters of the prepared photocatalysts, and as a result, their photocatalytic efficiency. The highest hydrogen evolution ratio was observed for DAP/Cu and DAP/Ag/Cu among metallic and bimetallic photocatalysts, respectively. The role of Cu is connected with the fact that the generated Schottky barrier is higher than that for Ag and consequently the transfer and trapping of photogenerated electrons by metal is higher, which influences the higher hydrogen generation rate. The deposition of Ag on the surface of Cu (DAP/Cu/Ag) is responsible for the inhibition of proton adsorption on the Cu surface and, as the result, a lower rate of hydrogen evolution. All metallic and bimetallic photocatalysts absorb visible light. Photoabsorption properties depend on the type of metal and its configuration on the DAP surface. Cu NPs mainly form small nanoclusters which are uniformly distributed on the DAP surface. Ag forms large polydispersed NPs. The aggregation of Ag NPs was confirmed by the broad LSPR peak of silver.

Modification of DAP with silver and copper significantly enhanced photocatalytic activity in the UV/vis range. It was found, on the basis of the oxidative decomposition of acetic acid, that this improvement of activity can be justified by possible heterojunctions between copper/silver oxides and titanium dioxide which can be responsible for inhibition of the recombination of charge carriers, together with the formation of the Schottky barrier. Similarly as was found for an anaerobic reaction system, morphology of bimetallic deposits is an important issue which influences photocatalytic activity.

DAP/Ag showed the highest visible light activity, higher than DAP/Cu and other bimetallic samples. In the case of DAP/Cu, copper is mainly in the form of Cu_2O and its heterojunction with titania is not preferred for visible light activity as TiO_2/CuO. Lower photocatalytic activity of bimetallic samples can possibly be explained by electron sinking in NPs of the second metal instead of being transferred via titania to adsorbed oxygen, which indirectly supports the mechanism of action of plasmonic photocatalysts by electron transfer rather than energy transfer.

It has been shown that the morphology of plasmonic photocatalysts is a key factor for photocatalytic activity under both UV and visible light irradiation. It is proposed that by morphology arrangement an efficient photocatalyst with the ability of working under the overall solar spectrum could be prepared. Although interesting results on the photocatalytic performance of anatase titania have been obtained, they need further study for clarification of phenomena observed, especially on the mechanism of electron transfer/recombination. Particle shape engineering together with the concept of plasmonic photocatalysts is a perspective area of design of new photocatalytic materials dedicated for selective reaction systems and working under the overall solar spectrum. The expected high photocatalytic efficiency of morphologically controlled nanoparticulate plasmonic systems can significantly contribute to the extension of photocatalysis applicability.

Acknowledgments

This research was funded by the Grand Challenges Explorations Grant (GCE R8, OPP1060234) from the Bill and Melinda Gates Foundation.

References

1. R. Abe, "Recent progress on photocatalytic and photoelectrochemical water splitting under visible light irradiation," *J. Photoch. Photobio. C* **11**(4), 179–209 (2010).
2. S. Licht, "Solar water splitting to generate hydrogen fuel: photothermal electrochemical analysis," *J. Phys. Chem. B* **107**(18), 4253–4260 (2003).
3. P. V. Kamat, "Meeting the clean energy demand: nanostructure architectures for solar energy conversion," *J. Phys. Chem. C* **111**(7), 2834–2860 (2007).
4. A. Zaleska, "Doped-TiO_2: a review," *Recent Pat. Eng.* **2**, 157–164 (2008).
5. M. R. Hoffmann et al., "Environmental applications of semiconductor photocatalysis," *Chem. Rev.* **95**(1), 69–96 (1995).
6. A. Fujishima and K. Honda, "Electrochemical photolysis of water at a semiconductor electrode," *Nature* **238**(5358), 37–38 (1972).
7. P. Pichat, "A brief survey of the potential health risks of TiO_2 particles and TiO_2-containing photocatalytic or non-photocatalytic materials," *J. Adv. Oxid. Technol.* **13**(3), 238–246 (2010).
8. B. Ohtani et al., "Titanium(Iv) oxide photocatalyst of ultra-high activity for selective N-cyclization of an amino-acid in aqueous suspensions," *Chem. Phys. Lett.* **242**(3), 315–319 (1995).
9. R. Beranek and H. Kisch, "Tuning the optical and photoelectrochemical properties of surface-modified TiO_2," *Photochem. Photobiol. Sci.* **7**(1), 40–48 (2008).
10. J. Kuncewicz et al., "Visible light driven photocatalysis in chromate(VI)/TiO_2 systems-improving stability of the photocatalyst," *Catal. Today* **161**(1), 78–83 (2011).
11. M. Janczarek et al., "Transparent thin films of Cu-TiO_2 with visible light photocatalytic activity," *Photochem. Photobiol. Sci.* **14**(3), 591–596 (2015).
12. R. Asahi et al., "Visible-light photocatalysis in nitrogen-doped titanium oxides," *Science* **293**(5528), 269–271 (2001).
13. T. Ohno et al., "Preparation of S-doped TiO_2 photocatalysts and their photocatalytic activities under visible light," *Appl. Catal. A* **265**(1), 115–121 (2004).
14. J. Kuncewicz and B. Ohtani, "Titania photocatalysis through two-photon band-gap excitation with built-in rhodium redox mediator," *Chem. Commun.* **51**(2), 298–301 (2015).
15. Y. Nakano et al., "Band-gap narrowing of TiO_2 films induced by N-doping," *Physica B* **376-377**, 823–826 (2006).
16. W. Macyk et al., "Titanium(IV) complexes as direct TiO_2 photosensitizers," *Coord. Chem. Rev.* **254**(21–22), 2687–2701 (2010).
17. W. Macyk and H. Kisch, "Photosensitization of crystalline and amorphous titanium dioxide by platinum(IV) chloride surface complexes," *Chem. Eur. J.* **7**(9), 1862–1867 (2001).
18. D. Mitoraj and H. Kisch, "On the mechanism of urea-induced titania modification," *Chem. Eur. J.* **16**, 261–269 (2010).

19. B. Kraeutler and A. J. Bard, "Heterogeneous photocatalytic preparation of supported catalysts. Photodeposition of platinum on TiO_2 powder and other substrates," *J. Am. Chem. Soc.* **100**, 4317–4318 (1978).
20. B. Ohtani et al., "Photocatalytic reaction of neat alcohols by metal-loaded titanium(IV) oxide particles," *J. Photochem. Photobiol. A* **70**(3), 265–272 (1993).
21. P. Pichat et al., "Photocatalytic hydrogen production from aliphatic alcohols over a bifunctional platinum on titanium dioxide catalyst," *Nouv. J. Chim.* **5**(12), 627–636 (1981).
22. M. Koudelka, J. Sanchez, and J. Augustynski, "Electrochemical and surface characteristics of the photocatalytic platinum deposits on TiO_2," *J. Phys. Chem.* **86**, 4277–4280 (1982).
23. A. Sclafani and J.-M. Herrmann, "Influence of metallic silver and of platinum-silver bimetallic deposits on the photocatalytic activity of titania (anatase and rutile) in organic and aqueous media," *J. Photochem. Photobiol. A* **113**(2), 181–188 (1998).
24. D. B. Ingram and S. Linic, "Water splitting on composite plasmonic-metal/semiconductor photoelectrodes: evidence for selective plasmon-induced formation of charge carriers near the semiconductor surface," *J. Am. Chem. Soc.* **133**, 5202–5205 (2011).
25. I.-K. Ding et al., "Plasmonic dye-sensitized solar cells," *Adv. Energy Mater.* **1**, 52–57 (2011).
26. K. Ueno and H. Misawa, "Surface plasmon-enhanced photochemical reactions," *J. Photoch. Photobio. C* **15**, 31–52 (2013).
27. Y. Tian and T. Tatsuma, "Mechanisms and applications of plasmon-induced charge separation at TiO_2 films loaded with gold nanoparticles," *J. Am. Chem. Soc.* **127**(20), 7632–7637 (2005).
28. E. Kowalska, R. Abe, and B. Ohtani, "Visible light-induced photocatalytic reaction of gold-modified titanium(IV) oxide particles: action spectrum analysis," *Chem. Commun.* (2), 241–243 (2009).
29. A. Furube et al., "Ulltrafast plasmon-induced electron transfer from gold nanodots into TiO_2 nanoparticles," *J. Am. Chem. Soc.* **129**(48), 14852–14853 (2007).
30. I. Caretti et al., "Light-induced processes in plasmonic gold/TiO_2 photocatalysts studied by electron paramagnetic resonance," *Top. Catal.* **58**(12–13), 776–782 (2015).
31. J. B. Priebe et al., "Solar hydrogen production by plasmonic Au-TiO_2 catalysts: Impact of synthesis protocol and TiO_2 phase on charge transfer efficiency and H_2 evolution rates," *ACS Catal* **5**(4), 2137–2148 (2015).
32. L. J. Brennan et al., "Hot plasmonic electrons for generation of enhanced photocurrent in gold-TiO_2 nanocomposites," *Nanoscale Res. Lett.* **10**, 1–12 (2015).
33. Z. Liu et al., "Plasmon resonance enhancement of photocatalytic water splitting under visible illumination," *Nano Lett.* **11**, 1111–1116 (2011).
34. S. K. Cushing et al., "Photocatalytic activity enhanced by plasmonic resonant energy transfer from metal to semiconductor," *J. Am. Chem. Soc.* **134**(36), 15033–15041 (2012).
35. Z. W. She et al., "Janus Au-TiO_2 photocatalysts with strong localization of plasmonic near fields for efficient visible-light hydrogen generation," *Adv. Mater.* **24**, 2310–2314 (2012).
36. X. Chen et al., "Visible-light-driven oxidation of organic contaminants in air with gold nanoparticle catalysts on oxide supports," *Angew. Chem. Int. Ed.* **47**, 5353–5356 (2008).
37. C. J. Wang et al., "Visible light plasmonic heating of Au-ZnO for the catalytic reduction of CO_2," *Nanoscale* **5**(15), 6968–6974 (2013).
38. W. B. Hou et al., "Photocatalytic conversion of CO_2 to hydrocarbon fuels via plasmon-enhanced absorption and metallic interband transitions," *ACS Catal.* **1**(8), 929–936 (2011).
39. D. Tsukamoto et al., "Gold nanoparticles located at the interface of anatase/rutile TiO_2 particles as active plasmonic photocatalysts for aerobic oxidation," *J. Am. Chem. Soc.* **134**(14), 6309–6315 (2012).
40. S. Mukherjee et al., "Hot electrons do the impossible: plasmon-induced dissociation of H_2 on Au," *Nano Lett.* **13**(1), 240–247 (2013).
41. A. Zielińska-Jurek et al., "Preparation and characterization of monometallic (Au) and bimetallic (Ag/Au) modified-titania photocatalysts activated by visible light," *Appl. Catal. B-Environ.* **101**(3–4), 504–514 (2011).
42. E. Kowalska, S. Rau, and B. Ohtani, "Plasmonic titania photocatalysts active under UV and visible-light irradiation: Influence of gold amount, size, and shape," *J. Nanotechnol.* **2012**, 361853 (2012).

43. P. A. DeSario et al., "Plasmonic enhancement of visible-light water splitting with Au-TiO_2 composite aerogels," *Nanoscale* **5**(17), 8073–8083 (2013).
44. Y. Horiguchi et al., "Preparation of gold/silver/titania trilayered nanorods and their photocatalytic activities," *Langmuir* **30**(3), 922–928 (2014).
45. S. K. Cushing and N. Q. Wu, "Progress and perspectives of plasmon-enhanced solar energy conversion," *J. Phys. Chem. Lett.* **7**(4), 666–675 (2016).
46. B. Ohtani et al., "What is Degussa (Evonik) P25? Crystalline composition analysis, reconstruction from isolated pure particles and photocatalytic activity test," *J. Photoch. Photobio. A* **216**(2–3), 179–182 (2010).
47. A. Markowska-Szczupak et al., "The effect of anatase and rutile crystallites isolated from titania P25 photocatalyst on growth of selected mould fungi," *J. Photoch. Photobio. B* **151**, 54–62 (2015).
48. E. Kowalska et al., "Silver-modified titania with enhanced photocatalytic and antimicrobial properties under UV and visible light irradiation," *Catal. Today* **252**, 136–142 (2015).
49. A. Zielinska et al., "Silver-doped TiO_2 prepared by microemulsion method: Surface properties, bio- and photoactivity," *Sep. Purif. Technol.* **72**, 309–318 (2010).
50. E. Kowalska et al., "Development of plasmonic photocatalysts for environmental application," *Adv. Sci. Tech.* **93**, 174–183 (2014).
51. X. Q. Qiu et al., "Hybrid Cu_xO/TiO_2 nanocomposites as risk-reduction materials in indoor environments," *ACS Nano* **6**(2), 1609–1618 (2012).
52. O. Baghriche et al., "Effect of the spectral properties of TiO_2, Cu, TiO_2/Cu sputtered films on the bacterial inactivation under low intensity actinic light," *J. Photochem. Photobiol. A* **251**, 50–56 (2013).
53. S. Rtimi et al., "TiON and TiON-Ag sputtered surfaces leading to bacterial inactivation under indoor actinic light," *J. Photochem. Photobiol. A* **256**, 52–63 (2013).
54. M. Janczarek, E. Kowalska, and B. Ohtani, "Decahedral-shaped anatase titania photocatalyst particles: synthesis in a newly developed coaxial-flow gas-phase reactor," *Chem. Eng. J.* **289**, 502–512 (2016).
55. Z. S. Wei, E. Kowalska, and B. Ohtani, "Enhanced photocatalytic activity by particle morphology: preparation, characterization, and photocatalytic activities of octahedral anatase titania particles," *Chem. Lett.* **43**(3), 346–348 (2014).
56. E. Kowalska and S. Rau, "Photoreactors for wastewater treatment: a review," *Recent Pat. Eng.* **4**(3), 242–266 (2010).
57. E. Kowalska et al., "Visible-light-induced photocatalysis through surface plasmon excitation of gold on titania surfaces," *Phys. Chem. Chem. Phys.* **12**(10), 2344–2355 (2010).
58. E. Kowalska et al., "Mono- and bi-metallic plasmonic photocatalysts for degradation of organic compounds under UV and visible light irradiation," *Catal. Today* **230**, 131–137 (2014).
59. Z. Wei et al., "Morphology-dependent photocatalytic activity of octahedral anatase particles prepared by ultrasonication-hydrothermal reaction of titanates," *Nanoscale* **7**(29), 12392–12404 (2015).
60. H. Reiche, W. W. Dunn, and A. J. Bard, "Heterogeneous photocatalytic and photosynthetic deposition of copper on titanium dioxide and tungsten(VI) oxide powders," *J. Phys. Chem.*, **83**(17), 2248–2251 (1979).
61. J.-M. Herrmann, J. Disdier, and P. Pichat, "Photoassisted platinum deposition on TiO_2 powder using various platinum complexes," *J. Phys. Chem.* **90**, 6028–6034 (1986).
62. S. Nishimoto et al., "Photoinduced oxygen formation and silver metal deposition in aqueous solutions of various silver salts by suspended titanium dioxide powder," *J. Chem. Soc.* **79**(11), 2685–2694 (1983).
63. S. Zheng et al., "Titania modification with ruthenium(II) complex and gold nanoparticles for photocatalytic degradation of organic compounds," *Photochem. Photobiol. Sci.* **15**, 69–79 (2016).
64. Z. Wei et al., "Enhanced photocatalytic activity of octahedral anatase particles prepared by hydrothermal reaction," *Catal. Today* (2016) (in press).

65. Z. Wei et al., "Noble metal-modified octahedral anatase titania particles with enhanced activity for decomposition of chemical and microbiological pollutants," *Chem. Eng. J.* (2016) (in press).
66. W. M. Sachtler and G. J. H. Dorgelo, "Surface of copper-nickel alloy films. I. Work function and phase composition," *J. Catal.* **4**(6), 654–664 (1965).
67. M. Chelvayohan and C. H. B. Mee, "Work function measurements on (110), (100) and (111) surfaces of silver," *J. Phys. C: Solid State Phys.* **15**(10), 2305–2312 (1982).
68. G. Fazio, L. Ferrighi, and C. Di Valentin, "Spherical versus faceted anatase TiO_2 nanoparticles: a model study of structural and electronic properties," *J. Phys. Chem. C* **119**(35), 20735–20746 (2015).
69. G. A. Hope and A. J. Bard, "Platinum/titanium dioxide (rutile) interface. Formation of ohmic and rectifying junctions," *J. Phys. Chem.* **87**, 1979–1984 (1983).
70. J. G. Mavroides et al., "Photoelectrolysis of water in cells with TiO_2 anodes," *Mater. Res. Bull.* **10**(10), 1023–1030 (1975).
71. T. Ioannides and X. E. Verykios, "Charge transfer in metal catalysts supported on doped TiO_2: a theoretical approach based on metal-semiconductor contact theory," *J. Catal.* **161**(2), 560–569 (1996).
72. A. L. Linsebigler, G. Lu, and J. T. Yates Jr., "Photocatalysis on TiO_2 surfaces: principles, mechanisms, and selected results," *Chem. Rev.* **95**, 735–758 (1995).
73. H. K. Wang et al., "Ag-Cu bimetallic nanoparticles prepared by microemulsion method as catalyst for epoxidation of styrene," *J. Nanomater.* **2012**, 4 (2012).
74. S. M. Skogvold et al., "Electrochemical properties of silver-copper alloy microelectrodes for use in voltammetric field apparatus," *Anal. Bioanal. Chem.* **384**(7–8), 1567–1577 (2006).
75. N. Nilius, N. Ernst, and H. Freund, "On energy transfer processes at cluster-oxide interfaces: silver on titania," *Chem. Phys. Lett.* **349**(5-6), 351–357 (2001).
76. V. Mizeikis, E. Kowalska, and S. Juodkazis, "Resonant, localization, enhancement, and polarization o optical fields in nano-scale interface regions for photo-catalytic application," *J. Nanosci. Nanotechnol.* **11**, 2814–2822 (2011).
77. M. Muniz-Miranda et al., "Characterization of copper nanoparticles obtained by laser ablation in liquids," *Appl. Phys. A* **110**(4), 829–833 (2013).
78. S. Ye et al., "Photochemically grown silver nanodecahedra with precise tuning of plasmonic resonance," *Nanoscale* **7**(29), 12706–12712 (2015).
79. V. Mizeikis et al., "Frequency- and polarization-dependent optical response of asymmetric spheroidal silver nanoparticles on dielectric substrate," *Phys. Status Solidi RRL* **4**(10), 268–270 (2010).
80. A. Zielinska-Jureka et al., "The effect of nanoparticles size on photocatalytic and antimicrobial properties of Ag-Pt/TiO_2 photocatalysts," *Appl. Surf. Sci.* **353**, 317–325 (2015).
81. M. G. Mendez-Medrano et al., "Surface modification of TiO_2 with Ag nanoparticles and CuO nanoclusters for applications in photocatalysis," *J. Phys. Chem. C* **120**, 5143–5154 (2016).
82. B. Karabiyik, *Plasmonic Materials with Enhanced Photocatalytic and Antimicrobial Properties*, p. 62, Department of Inorganic Chemistry, Ulm University, Ulm, Germany (2014).
83. G. Colon et al., "Cu-doped TiO_2 systems with improved photocatalytic activity," *Appl. Catal., B* **67**(1-2), 41–51 (2006).
84. A. L. Luna et al., "Photocatalytic degradation of gallic acid over CuO-TiO_2 composites under UV/Vis LEDs irradiation," *Appl. Catal. A-Gen.* **521**, 140–148 (2016).
85. K. Siuzdak et al., "Preparation of platinum modified titanium dioxide nanoparticles with the use of laser ablation in water," *Phys. Chem. Chem. Phys.* **16**(29), 15199–15206 (2014).
86. J. G. Yu, X. J. Zhao, and Q. N. Zhao, "Effect of surface structure on photocatalytic activity of TiO_2 thin films prepared by sol-gel method," *Thin Solid Films* **379**(1–2), 7–14 (2000).
87. J. Reszczynska et al., "Lanthanide co-doped TiO_2: The effect of metal type and amount on surface properties and photocatalytic activity," *Appl. Surf. Sci.* **307**, 333–345 (2014).
88. J. T. Carneiro et al., "How gold deposition affects anatase performance in the photo-catalytic oxidation of cyclohexane," *Catal. Lett.* **129**(1-2), 12–19 (2009).

89. B. K. Min, W. T. Wallace, and D. W. Goodman, "Support effects on the nucleation, growth, and morphology of gold nano-clusters," *Surf. Sci.* **600**, L7 (2006).
90. J. Reszczynska et al., "Photocatalytic activity and luminescence properties of $RE3^{+}$-TiO_2 nanocrystals prepared by sol-gel and hydrothermal methods," *Appl. Catal. B* **181**, 825–837 (2016).
91. S. H. Szczepankiewicz, A. J. Colussi, and M. R. Hoffmann, "Infrared spectra of photoinduced species on hydroxylated titania surfaces," *J. Phys. Chem. B* **104**(42), 9842–9850 (2000).
92. S. Rtimi et al., "Coupling of narrow and wide band-gap semiconductors on uniform films active in bacterial disinfection under low intensity visible light: implications of the interfacial charge transfer (IFCT)," *J. Hazard. Mater.* **260**, 860–868 (2013).
93. Z. B. Hai et al., "Modification of TiO_2 by bimetallic Au-Cu nanoparticles for wastewater treatment," *J. Mater. Chem. A* **1**(36), 10829–10835 (2013).
94. Z. B. Hai et al., "Radiolytic synthesis of Au-Cu bimetallic nanoparticles supported on TiO_2: Application in photocatalysis," *New J. Chem.* **38**(11), 5279–5286 (2014).

Marcin Janczarek received his PhD in chemical technology from Gdansk University of Technology, Poland, in 2005. He also worked at the University of Erlangen-Nürnberg, Germany (2003–2004), and at Hokkaido University, Japan (2011–2013). He is an assistant professor at Gdansk University of Technology. His current research interests include heterogeneous photocatalysis, materials engineering, and technologies for purification of water and air.

Zhishun Wei received his MS degree in nanomaterials and nanotechnology from the Graduate School of Material Science and Engineering, Sichuan University, China, in 2010, and his PhD in photocatalysis from the Graduate School of Environmental Science, Hokkaido University, Japan, in 2014. He is a postdoctoral researcher in the Institute for Catalysis at Hokkaido University. His current research interests include photocatalysis, nanomaterial, and material chemistry.

Maya Endo received her BSc and MSc degrees in chemistry from Hokkaido University. She is a research fellow in the Institute for Catalysis at Hokkaido University. Her current research interests include plasmonic photocatalysts for antimicrobial activity.

Bunsho Ohtani has been a professor in the Institute for Catalysis (previously Catalysis Research Center), Hokkaido University, since 1998, focusing on fundamentals of heterogeneous photocatalysis. He started his research career as an assistant professor in Kyoto University after getting his PhD in the university in 1985 and was promoted to associate professor in the Graduate School of Science, Hokkaido University, in 1996.

Ewa Kowalska received her PhD in chemical technology from Gdansk University of Technology, Poland, in 2004. She is an associate professor and a leader of the Research Cluster for Plasmonic Photocatalysis in the Institute for Catalysis at Hokkaido University. After completing a Japan Society for the Promotion of Science fellowship (2005–2007), GCOE postdoctoral fellowships (2007–2009) in Japan, and Marie Curie fellowships in France (2002–2003) and in Germany (2009–2012), she joined the Institute for Catalysis as an associate professor in 2012. Her current work focuses on the heterogeneous photocatalysis, environmental protection, plasmonic nanomaterials, and antimicrobial properties.